Diffusion suppression control of a free jet at a medium Reynolds number with transverse vibration of inflow

K. Tsujimoto[1], T. Tanoue[1], T. Ando[1] and M. Takahashi[1]

[1]Division of Mechanical Engineering, Graduate School of Engineering, Mie University, Japan

Keywords: Active flow control; Free jet; Diffusion suppression; Deep reinforcement learning; Open-loop control

Abstract. A significant amount of research has been conducted on the enhancement of jet-induced mixing and diffusion. However, there is little knowledge of techniques to suppress the diffusion of jets, and machine learning control is considered promising for creating new control methods. However, at present, most flow fields targeted by machine learning are low Reynolds numbers. In medium- and high-Reynolds-number flow fields, the degrees of freedom increase, making the control difficult. In this paper, we develop a computational code in Fortran for both the flow field and machine learning for a two-dimensional jet with a Reynolds number of 1500 and address the problem of suppressing the diffusion of the jet. We focus on a method of vibrating the jet in the transverse direction as a control method for suppressing the diffusion of the jet and perform both open-loop control with a fixed vibration frequency and DRL(deep reinforcement learning) using the DDPG (deep deterministic policy gradient) method, apply these results to a three-dimensional planar jet, and demonstrate the overall feasibility of the proposed control method for effectively suppressing jet turbulence and controlling mixing.

1. Introduction

Free jets are utilized as a key technology for enhancing the mixing and heat transfer. There is growing interest in energy conservation as a green technology and airflow control related to COVID-19 countermeasures. These areas require the development of flow control methods that are more precise than conventional methods. Many existing control methods aim to achieve significant jet dispersion downstream to actively promote mixing. Numerous passive and active jet control methods have been proposed. In the case of active control, the focus has been on actively utilizing the flow instability within the jet. For axisymmetric jets, the unstable modes characterizing large-scale structures in the nozzle proximity are the azimuthally uniform axisymmetric mode (axisymmetric mode: a mode in which the jet repeatedly contracts and expands in the axial direction) and helical mode, with these two dominating modes, as confirmed by the linear stability analysis results. By exciting these modes, jet control such as bifurcating and blooming modes has been experimentally verified[1]. Active control has also been examined in direct numerical simulations (DNS), and strong jet diffusion has been reproduced[2,3]. Because active control inevitably requires setting control parameters manually, to further improve performance, it is necessary to efficiently search for control parameters and find those that respond flexibly to changes in the flow-field state. On the other hand, research on methods to suppress jet mixing is limited, and some studies have been conducted, such as turbulence suppression by acoustic excitation at high frequencies[4], reduction of Reynolds stress by vibration of the mixing layer[5], and the discovery of velocity distribution profiles at the inlet that suppress turbulence by machine learning[6]. Recently, there has been growing interest in machine learning[8]. Among the fields of machine learning, reinforcement learning (RL), which can handle unsupervised problems without a clear solution, and deep reinforcement learning (DRL), which incorporates neural networks, can learn actions that maximize the control effects (rewards) as optimal control. This offers the potential to develop effective control methods by applying these to conventional active controls. As an example of this potential, Rabault et al.[7] adopted proximal policy optimization (PPO)[9], which is a control scheme in DRL, and achieved beneficial results in reducing the drag around a cylinder. The study by Rabault et al. has become a milestone for active flow control around cylinders. Since then, efforts involving the PPO for active flow control have been actively pursued. Koizumi et al.[10] adopted the deep deterministic policy gradient (DDPG)[11] method in DRL to reduce the lift around a cylinder, revealing interesting characteristics. Inspired by this research, the authors applied a similar approach and demonstrated that a beneficial mixing performance in free jets can be achieved using DRL[12].

Building on the knowledge gained from low-Reynolds-number applications, this study focuses on a two-dimensional plane jet with a Reynolds number of 1500 and proposes a method to suppress turbulence in the jet by vibrating the inlet in the transverse direction. We perform both open-loop control with a fixed vibration frequency and DRL using the DDPG method, apply these results to a three-dimensional planar jet, and demonstrate the overall feasibility of the proposed control method for effectively suppressing jet turbulence and controlling mixing.

2. Numerical Method

*2.1 Governing equation and discretizatio*n

The non-dimensional governing equations (continuity equation and equation of motion) used in this study, under the assumption of an incompressible field, are presented in the following tensor notation:

$$\frac{\partial u_i}{\partial x_i} = 0 \tag{1}$$

$$\frac{\partial u_i}{\partial t} + h_i = -\frac{\partial p}{\partial x_i} + \frac{1}{\mathrm{Re}}\frac{\partial^2 u_i}{\partial x_j \partial x_j} \tag{2}$$

$$(h_i = \varepsilon_{ijk}\omega_j u_k,\ \omega_j : vorticity)$$

where u_i is the velocity component along x_i direction. When a rotational type is used for the convection term, p represents total pressure. Upon non-dimensionalization, using the nozzle width H as the representative length and jet center velocity V_0 in the main flow direction as the representative velocity, the Reynolds number becomes $\mathrm{Re} = V_0 H/\nu$ (ν: dynamic viscosity coefficient). The computational domain is rectangular, as shown in Figure 1, with the main flow direction defined as *y,* and the direction perpendicular to the main flow is defined as *x*. The domain is discretized using a sixth-order compact scheme[13] in the main flow direction and sine and cosine series in the directions perpendicular to the main flow. To remove the numerical instability caused by aliasing errors from the convection term, filtering is performed in the wavenumber space in the direction perpendicular to the main flow, whereas implicit filtering is applied in the main flow direction using the sixth-order compact scheme. The Adams-Bashforth method with third-order accuracy was used for time integration. After the Poisson equation for pressure is Fourier transformed, it becomes an independent differential equation for each wavenumber. By further applying a sixth-order compact difference approximation, a pentadiagonal matrix is obtained, which is then solved using a direct method. The convective outflow condition is used as the outflow boundary condition.

2.2 Calculation condition

If the distance from the central axis of the jet is *x*, and the inflow velocity profile V_p in the axial direction of the jet is assumed to be top-hat shaped[3], it is given by the following equation:

$$V_p(x) = \frac{V_0}{2} - \frac{V_0}{2}\tanh\left[\frac{1}{2}\frac{H}{\theta_0}\left(\frac{2x}{H} - \frac{H}{2x}\right)\right] \tag{3}$$

where V_0 is the central velocity of the jet in the main flow direction; θ_0 is the initial momentum thickness; and H is the jet width. The parameters is set to $H/\theta_0 = 40$ based on the literature [3]. As shown in figure 1, the size of the computational domain is $(L_x, L_y) = (20H, 30H)$, and the number of grids is $(N_x, N_y) = (256, 201)$. The jet inlet velocity V_{inf} is vibrated in a direction perpendicular to the main flow direction.

$$V_{inf}(x) = V_p[x - A_0\sin(2\pi f t)] \tag{4}$$

where A_0 and f denote the vibration amplitude and frequency, respectively.

In the DDPG method, a reinforcement learning algorithm that uses deep neural networks to learn the optimal control policies employed in this study, control is achieved by modulating the frequency f to

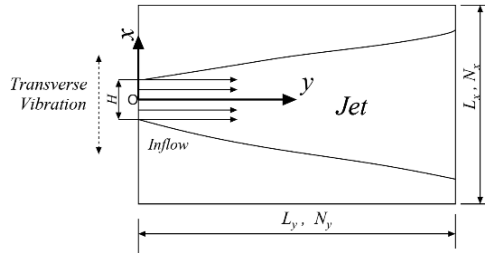

Figure 1. Transvers vibration control.

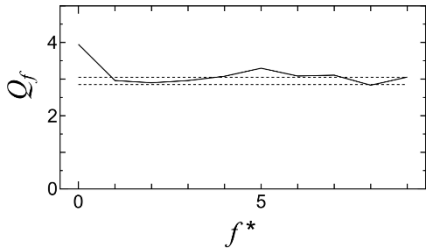

Figure 3. Flow rate Q_f at different control frequencies.

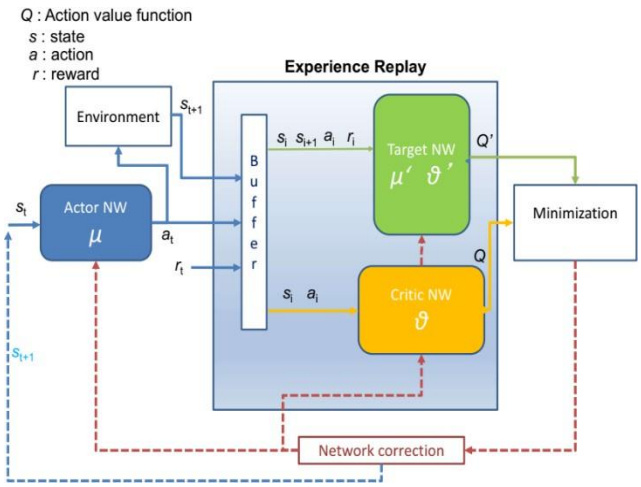

Figure 2. DDPG Algorithm.

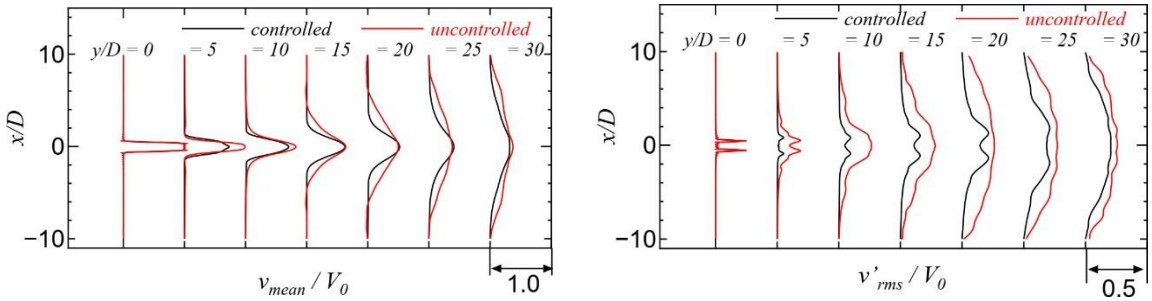

Figure 4. Distribution of mean main flow velocity, v_{mean}, and velocity fluctuation intensity, v'_{rms}.

achieve a smooth vibration. Specifically, the upper limit of the frequency is set as f_0, and the frequency is defined as $f = f_0\ (a + 1)$, where $-1 \leq a \leq 1$, and action a is determined through machine learning. In this study, both DDPG and Computational Fluid Dynamics (CFD) simulations are coded entirely in FORTRAN.

3. Results

3.1 *Open control for two-dimensional jet*

The entrainment characteristics of a jet, representing the mixing state of the jet, are evaluated using Q_f, the integrated velocity at the downstream cross-section.

$$Q_f = \int_{-H_x/2}^{H_x/2} v \, dx \tag{5}$$

Figure 3 shows the characteristics of the jet when $f^* = fH/V_0$ is varied in increments of 1. At low frequencies, Q_f decreases as the frequency increases. The width of the dashed line in the figure represents 5% of the maximum Q_f value. Considering that the dominant mode of the plane jet is approximately 0.25[14], it can be seen that the mixing performance becomes saturated at high frequencies. Here, for $f^* = 2$ as a representative value, the distribution of the mean velocity v_{mean} and its fluctuation intensity v'_{rms} in the main flow direction are shown in figures 4. The mean velocity distribution, with and without control, spreads laterally downstream, which is characteristic of jets;

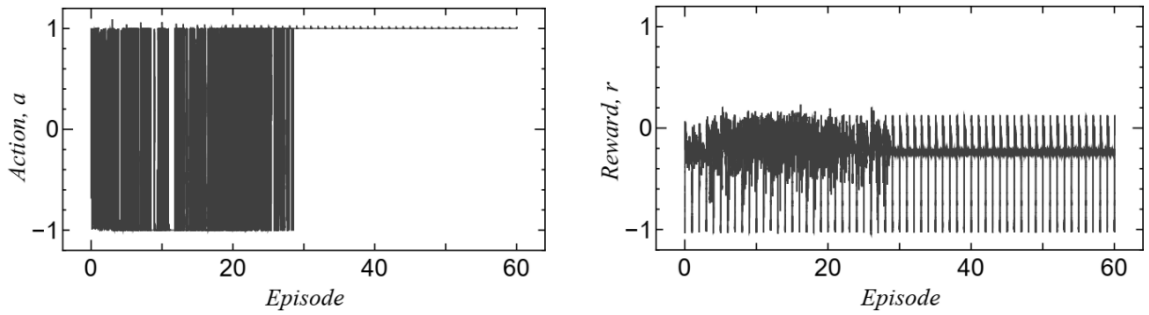

Figure 5. Action *a* and reward *r* in DRL.

downstream from approximately y/H = 10, it can be seen that the control suppresses diffusion. The velocity fluctuation intensity exhibits two peak values owing to the strong shear layer at the outer edge of the jet. When controlled, these two peaks remain relatively far downstream. In other words, under vibration control, the generation of K-H instabilities and formation of large-scale vortex structures are suppressed. It also does not lead to an increase in the Reynolds stress, which reduces the turbulence. Thus, the proposed vibration control is an effective method for suppressing turbulence.

3.2 *Deep Reinforcement Learning Control of Two-Dimensional Je*t

Several deep reinforcement learning (DRL) methods have been proposed; however, because flow control problems typically involve continuous action spaces, unlike discrete action spaces found in games, we adopt the DDPG method, as illustrated in figure 2. DDPG is a model-free off-policy algorithm that can handle continuous action spaces, making it suitable for flow control. As shown in figure 2, reinforcement learning combines the concepts of environment (state), action, and reward for learning. In other words, in a given environment, actions are selected based on a policy, and states and rewards are obtained. The environment changes the state based on the actions taken, and rewards are provided accordingly. A policy that maximizes rewards is found through the rewards obtained by actions. In this study, the action is the vibration frequency and the state is the velocity at the monitoring locations. Although not mentioned in the algorithm in Figure 2, there are several parameters to consider, such as the number of layers and nodes in the neural network, choice of activation functions, method of introducing the noise required for exploration, discount factor in the action-value function Q, and determination of the reward structure. These parameters must be carefully selected to avoid situations in which the learning process becomes unstable or fails to converge. For example, inappropriate noise introduction can lead to excessive exploration, which hinders the convergence. A temporal delay exists between the states and actions. Koizumi et al. [9] pointed out the necessity of a time-delayed Markov decision process and proposed a method for incorporating time-delayed states and actions into the current state. In this study, instead of explicitly considering the time delay, 50 observation points are arranged downstream along the jet center line, with learning occurring at each time step of the CFD simulation. This approach allows the agent to observe the effects of its actions over a spatial extent. 10,000 time steps of calculation are allocated for each learning episode, and the entire learning process is completed in approximately 60 episodes. There are 64 states extracted from the replay buffer. The neural network consists of an actor network, where the input layer has 50 nodes, the output layer has one node for the action, the first hidden layer contains 200 nodes in a fully connected layer, and the second layer has 200 nodes in a fully connected layer. The tanh function is selected as the activation function because it outputs values within a bounded range. The critic network input layer has 50 nodes for the state and one node for the action. Similarly, the 200 nodes fully connected layer serves as the hidden layer, with a linear function as the activation function. The goal of the reward is to prevent fluctuations in the jet and reduce entrainment. It is defined by the following equation:

$$r = 1.0 - (v'_{mon} / v'_{mon0})^2$$

(a) Iso-surface of second invariance velocity gradient tensor from plane view.

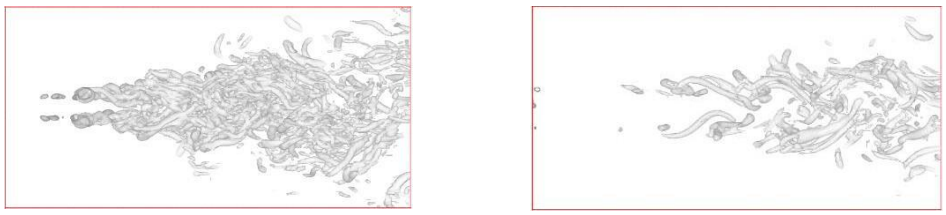

(b) Iso-surface of second invariance velocity gradient tensor from side view.

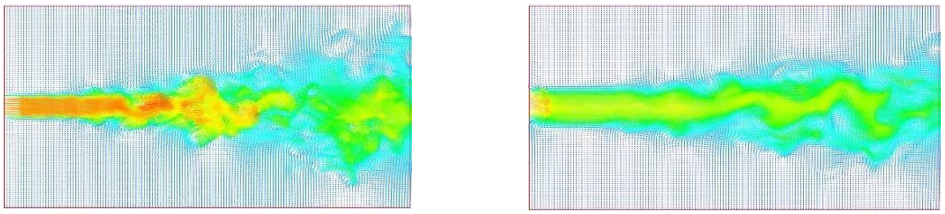

(c) Velocity vector plots on *x*-*y* plane.

Figure 6. Instantaneous flow field, left: uncontrolled; right: controlled.

where v'_{mon} is the instantaneous main flow velocity fluctuation at $y = 1.5H$ averaged over the interval ($-0.75H < x < 0.75H$). v'_{mon0} is the value of v'_{mon} in the case without control. As shown in figures 5, up to episode 28, the control behavior exhibits significant oscillations, but after that, it transitions to a very stable state. The change in reward at this time follows the changes in actions. Recently, Wang et al. [15] worked on reducing the drag of a three-dimensional cylinder at high Reynolds numbers by placing a small rotating cylinder outside the main cylinder and controlling its rotational speed using machine learning. Consequently, a convergent solution with a constant rotation speed was obtained after approximately 40 episodes. It is important to note that the use of machine learning does not inherently lead to fluctuating solutions, and stable solutions with characteristics similar to those found by Wang et al. are also obtained in this study.

3.3 *Transverse Vibration Control of Three-Dimensional Jet*

Using this control method, suppression effects are demonstrated even at a constant frequency, based on the results of the open-loop control. However, it is necessary to confirm whether vibration control works for the three-dimensional turbulence behaviour at moderate Reynolds numbers. Here, the results of the open-loop control at $f^* = 2.0$ from the previous results are shown. The computational domain and grid numbers are given by (H_x, H_y, H_z) = (10H, 20H, 5H) and (N_x, N_y, N_z) = (128, 150, 64), respectively. Instantaneous coherent vortices and velocity vector plots are shown in figures 6. In the case without control, large-scale roll vortices, which are characteristic of plane jets, are formed near the nozzle, and a complex interaction of the rib vortex structures in the main flow direction can be seen. However, when control is applied, the generation of vortices is suppressed; specifically, the roll vortices are weakened and the interaction of the rib vortices is reduced. The vector plot reflects suppressed jet diffusion. Figures 7 shows the distribution of the mean velocity in the main flow direction and turbulence energy T_k ($= \frac{1}{2}\overline{u'_i u'_i}$) . The diffusion of the jet is suppressed by the control; however, the effect is weaker than that of

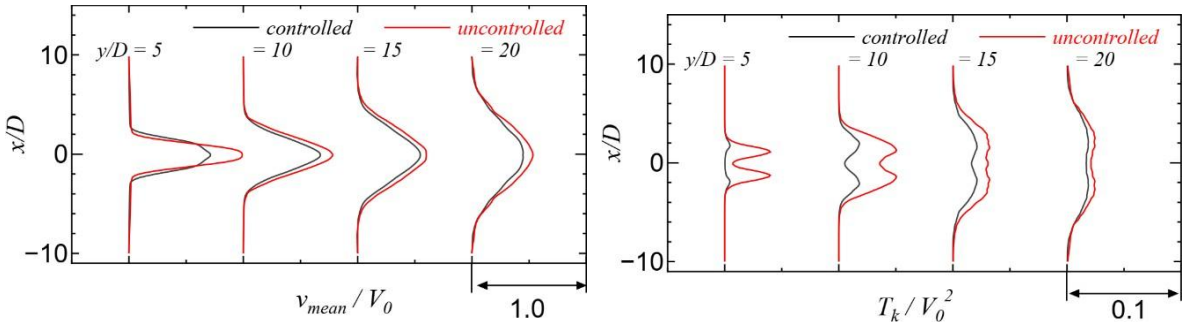

Figures 7. Distribution of mean main flow velocity, v_{mean}, and turbulent kinetic energy T_k in 3D simulations

the 2D computations. Corresponding to figures 6 (a) and (b), it can be observed that turbulence is significantly suppressed in the upstream region.

4. Concluison

Using DNS, we addressed the suppression control of a two-dimensional (2D) jet with transverse vibration. The results of the open-loop control revealed that a constant suppression effect appears regardless of the frequency once a threshold frequency of approximately f^*=1 is exceeded. Furthermore, through DRL-based vibration control, it was verified that even when the frequency is modulated, the system converges to a constant frequency, which corresponds to the solution obtained from the open-loop control. Additionally, the results obtained from the 2D simulations were applied to a 3D flow field, and it was found that the proposed control method still demonstrates suppression effects. However, the suppression effect is smaller than that of the 2D simulations. Further investigation into DRL-based control for 3D flow fields, including optimization of the reward function and neural network architecture, warrants further investigation. Future work will focus on extending DRL control to 3D flows.

References

[1] Reynolds, W. C., Parekh, D. E., Juvet, P. J. D. and Lee, M. J. D. 'Bifurcating and Blooming Jets', Annu. Rev. Fluid Mech. (2003), pp.295-315.
[2] Hilgers, A. and Boersma, B. J. 'Optimization of turbulent jet mixing,' Fluid Dyn. Res., 29 (2001), pp.345-368.
[3] Silva, C. B. and Metais, O. 'Vortex control of bifurcating jets: A numerical study', Phys. Fluids, 14 (2002), pp.3798-3819.
[4] Zaman, K. B. M. Q., Hussain, A. K. M. F. 'Turbulence suppression in free shear flows by controlled excitation', J. Fluid Mech., 103 (1981), pp. 133-159.
[5] Kametani, Y., Kawagoe, M., Fukagata, K. 'Direct numerical simulation of a turbulent mixing layer with a transversely oscillate inflow', J. Fluid Sci. Tech., 10 (2015), 14-00292.
[6] Ito, Y., Hayashi Y., Iwano, K., Katagiri, T. 'Optimisation of initial velocity distribution of jets for entrainment and diffusion control using deep reinforcement learning', Int. J. Heat Mass Trans., 218 (2024), 124788.
[7]Brunton, S. L., Noack, B. R., and Koumoutsakos, P. Machine Learning for Fluid Mechanics', Annu. Rev. Fluid Mech., 52 (2020), pp. 477-508.
[8]Rabault, J., Kuchta, M., Jensen, A., and R$\acute{e}$glade, U. 'Artificial neural networks trained through deep reinforcement learning discover control strategies for active flow control', J. Fluid Mech., 865 (2019), pp. 281-302.
[9]Schulman, J., Wolski, F., Dhariwal, P., Radford, A., Klimov, O. 'Proximal policy optimization algorithms', (2017) arXiv:1707.06347.
[10] Koizumi, H.al.. Tsutsumi, S., and Shima, E. 'Feedback control of Karman vortex shedding from a cylinder using deep reinforcement learning', AIAA Paper (2018), No. 2018-3691.
[11] Lillicrap, T.P., Hunt, J.J., Pritzel, A., Heess, N., Erez, T., Tassa, Y., Silver, D., Wierstra, D. 'Continuous control with deep reinforcement learning', Int. Conf. Learn. Represent (2016) arXiv:1509.02971v5.
[12] Tsujimoto, K. and Tanoue, T. 'Mixing Enhancement of Free Jet using Deep Reinforcement Learning', Proc. 22nd Australasian Fluid Mechanics Conf. AFMC2020 (2020), 4 pages.
[13] Lele, S. K. 'Compact finite difference schemes with spectral-like resolution', J. Comp. Phys.,103 (1992), pp.16-42.
[14] Ho C-M, Huerre P. 'Perturbed free shear layers', Ann Rev Fluid Mech 16(1984), pp.365–424
[15] Wang, Z., Fan,D., Jiang, X.,Triantafyllou, M. S., Karniadakis, G. E. 'Deep reinforcement transfer learning of active control for bluff body flows at high Reynolds number', J. Fluid Mech., 973 (2023), A32.